

Multichannel Speech Enhancement by Raw Waveform-mapping using Fully Convolutional Networks

Chang-Le Liu¹, Szu-Wei Fu², You-Jin Lee², Yu Tsao², Jen-Wei Huang³, and Hsin-Min Wang²

¹National Taiwan University

²Academia Sinica, Taipei, Taiwan

³National Cheng-Kung University

ABSTRACT

In recent years, waveform-mapping-based speech enhancement (SE) methods have garnered significant attention. These methods generally use a deep learning model to directly process and reconstruct speech waveforms. Because both the input and output are in waveform format, the waveform-mapping-based SE methods can overcome the distortion caused by imperfect phase estimation, which may be encountered in spectral-mapping-based SE systems. So far, most waveform-mapping-based SE methods have focused on single-channel tasks. In this paper, we propose a novel fully convolutional network (FCN) with Sinc and dilated convolutional layers (termed SDFCN) for multichannel SE that operates in the time domain. We also propose an extended version of SDFCN, called the residual SDFCN (termed rSDFCN). The proposed methods are evaluated on two multichannel SE tasks, namely the dual-channel inner-ear microphones SE task and the distributed microphones SE task. The experimental results confirm the outstanding denoising capability of the proposed SE systems on both tasks and the benefits of using the residual architecture on the overall SE performance.

Index Terms—Multichannel speech enhancement, raw waveform mapping, fully convolutional network, Sinc convolutional filters, dilated fully convolutional filters, inner-ear microphones, distributed microphones.

1. INTRODUCTION

Speech-related applications for both human-human and human-machine interfaces have garnered significant attention in recent years. However, speech signals are easily distorted by additive or convolutional noises or recording devices, and such distortion constrains the achievable performance of these applications. To address this issue, numerous speech enhancement (SE) algorithms have been derived to improve the quality and intelligibility of distorted speech and are widely used as a preprocessor in speech-related applications, such as speech coding [1], [2], assistive hearing devices [3], [4], and automatic speech recognition (ASR) [5]. Generally speaking, SE methods can be divided into two categories. The first category adopts a single channel (also termed monaural) while the second category uses multiple microphones (also termed multichannel) to perform SE.

Traditional single-channel-based SE methods were derived based on the characteristics and statistical assumptions of clean

speech and noise signals. Well-known approaches include spectral-subtraction [6], the Wiener filter [7], [8], and the minimum mean square error (MMSE) [9]. Another category of successful SE approaches is subspace-based methods, which aim to separate noisy speech into two subspaces, one for clean speech and the other for noise components. The clean speech is then restored based on the information in the clean-speech subspace. Notable subspace techniques include generalized subspace approaches with prewhitening [10], the Karhunen-Loeve transform [11], and principal component analysis (PCA) [12].

In recent years, machine-learning-based algorithms have been popularly used in the SE field. Unlike traditional methods, a machine-learning-based SE approach generally prepares a denoising model in a data-driven manner without imposing strong statistical constraints. Well-known machine-learning-based models include nonnegative matrix factorization [13], compressive sensing [14], sparse coding [15], and robust principal component analysis (RPCA) [16]. More recently, deep learning models have been applied to the SE field. Owing to their outstanding nonlinear mapping capability, deep-learning-based SE methods have demonstrated notable performance improvements over traditional statistical methods and other machine-learning-based methods. Well-known deep-learning-based models include the deep denoising autoencoder (DDAE) [17], [18], deep fully connected networks [19]–[22], recurrent neural networks (RNNs) [23], [24], convolutional neural networks [25], [26], and long short-term memory (LSTM) [27]–[30].

Different from single-channel SE methods, the multichannel ones utilize information from plural channels to enhance the target speech signal. Among the multichannel SE methods, beamforming [31]–[33] is a popular method that exploits spatial information from multiple microphones to attenuate interference and noise signals. In addition to beamforming, other effective methods are based on a coherence algorithm that calculates the correlation of two input signals to estimate a filter to attenuate the interference components [34], [35]. Meanwhile, Li et al. proposed a method of using distributed-microphones for in-vehicle SE [36]. They argued the clean speech signals acquired by distributed-microphones are similar to each other while the noise signals acquired by distributed-microphones are irrelevant to each other. Therefore, the RPCA algorithm [16] is applied to the matrix formed by the acquired noisy signals from multiple channels to separate clean speech and noise components [36].

More recently, deep learning-based models also exhibit encouraging performance in multichannel SE tasks. Araki et al.

showed that multichannel audio features can effectively improve the performance of the denoising autoencoder (DAE) [37] based SE approach [38]. Wang and Wang proposed a deep learning-based time-frequency (T-F) masking SE method that estimates robust time delay of arrival over multiple singly-enhanced speech signals to obtain directional features and hence the beam-formed signals. The enhancement is carried out by combining spectral and directional features [39]. Although the abovementioned multichannel SE approaches have been able to provide satisfactory performance, they are performed in the frequency domain, i.e., they typically use the phase from the noisy input and require additional processing to convert the speech waveform into spectral features. To avoid imperfect phase estimation and reduce online processing, waveform-mapping-based audio signal processing methods have been developed. For example, in [40]–[44], a fully convolutional network (FCN) model was used to enhance on the noisy waveform to generate an enhanced waveform, and in [45], [46], the FCN model was used to separate a singing voice from mono or stereo music.

In the present work, we propose a novel fully convolutional network that incorporates Sinc convolutional filters (termed SincConv) and dilated convolutional filters, to perform multichannel SE in the time domain. Therefore, the model is called Sinc dilated FCN (termed SDFCN). In addition, we derive an extended system from the SDFCN system. The extended system structures a residual architecture in which SDFCN is used to estimate and compensate for the residual components of the enhanced speech from a primary SE model. Therefore, it is named residual SDFCN (termed rSDFCN). We evaluate the proposed models on two multichannel SE tasks: inner-ear microphones (termed the IEM-SE task) and distributed-microphones (termed the DM-SE task). For both tasks, the proposed SE models take inputs from multiple channels to generate a single-channel waveform with higher quality and intelligibility than individual noisy inputs. Two standardized metrics are used in the evaluation: short-time objective intelligibility (STOI) [47], [48] and perceptual estimation of speech quality (PESQ) [49]. In addition, we compare the speech recognition performance of the enhanced speech signals. Our experimental results confirm the outstanding denoising capability of the proposed SDFCN and rSDFCN models in both IEM-SE and DM-SE tasks and demonstrate the benefits of using the residual architecture on the overall SE performance.

The remainder of this paper is organized as follows. Section 2 reviews the related works. Section 3 presents the concept and architectures of the proposed SDFCN and rSDFCN models. Section 4 presents the experimental setup and results. Finally, Section 5 concludes this work.

2. RELATED WORKS

Given a clean speech signal \mathbf{x} , the degraded signal can be formulated as $\mathbf{y} = \mathbf{g}(\mathbf{x})$, where \mathbf{g} denotes the degradation function. The goal of SE is to find a function that maps \mathbf{y} to $\tilde{\mathbf{x}}$ and approximates \mathbf{x} as close as possible. In this section, we review related works, including the FCN-based waveform-mapping-based SE method, SincConv filters, and dilated convolutional filters.

2.1. Waveform-mapping-based SE

Previous studies have shown that the FCN model is suitable for waveform-mapping-based SE because the convolutional layers can more effectively characterize the local information of neighboring

input regions [40]. FCN is a modified convolutional neural network (CNN) model in which the fully connected layers in CNN are completely replaced by the convolutional layers, as shown in Fig. 1. In FCN, the relation between the output y_t and the connected hidden nodes \mathbf{h}_t can be represented by

$$y_t = \mathbf{v}^T \mathbf{h}_t \quad (1)$$

where $\mathbf{v} \in \mathbb{R}^{f \times 1}$ denotes a convolutional filter, and f is the size of the filter. Note that \mathbf{v} is shared in the convolution operation and is fixed for every output. Because the pooling step may reduce the precision of speech signal reconstruction, we did not apply any pooling operations (e.g., WaveNet [50]) to perform SE when using FCN. For more details about the structure of the FCN model applied to waveform-mapping-based SE, please refer to previous works [40], [41], and [50].

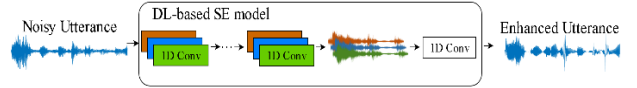


Fig. 1. A waveform-mapping-based SE system.

2.2. SincConv Filters

As mentioned above, convolutional filters are often used to process raw-waveforms. When the CNN model is too deep or the training data is insufficient, the filters of the first few layers may not be well learned because of the vanishing gradient issue. To overcome this issue, Ravanelli *et al.* recently proposed a novel convolutional architecture, called SincNet. Unlike conventional CNN models that learn all filters based on training data, SincNet predefines the filters of the first few layers to model the rectangular band-pass filter-banks in the frequency domain. Specifically, the filter function \mathbf{h}^w , which will be convolved with the input signal \mathbf{y} , can be written as follows:

$$\begin{aligned} \mathbf{h}_t^w &= \mathbf{h}_t \circ \mathbf{w}_t \\ \mathbf{h}_t &= 2f_{low}\text{sinc}(2\pi f_{low}t) - 2f_{high}\text{sinc}(2\pi f_{high}t), \\ \mathbf{w}_t &= 0.54 - 0.46\cos(2\pi t/L) \end{aligned} \quad (2)$$

where L is the filter length, and f_{low} and f_{high} are the low and high cutoff frequencies learned during training, respectively. Obviously, this architecture is much more efficient because each filter in the first layer only consists of two coefficients rather than L (the original filter length) coefficients. In [51], it was shown that SincNet converged faster in training and performed better in testing than CNN on a speaker recognition task when the input is raw speech waveform. A lower number of neurons enables SincNet to be well trained even on a limited training dataset [51].

2.3 Dilated convolution

Previous works, such as WaveNet [50], TasNet [52], and WaveGAN [53] showed that using a large temporal context window is important in waveform modeling. To efficiently take advantage of the long-range dependency of speech signals, dilated convolution is proposed in [54]. In [43], [50], and [54], the effectiveness of the dilated convolutional layers was shown to expand the receptive field exponentially (rather than linearly) with depth. Fig. 2 shows an example that demonstrates the concept of dilated fully convolutional filters. The input signal (I) is processed by a dilated convolutional block to generate the output signal (O).

The input sequence has 18 points. When using a one-dimensional fully convolutional filter to process the input signal, the number of receptive fields is 18. Meanwhile, when using a dilated fully convolutional block with filter sizes of 2, 3, and 3 and dilated rates of 1, 2, and 6, the receptive field is also 18. Compared to a single-layered FCN block, with the same size of receptive fields, the dilated fully convolutional block requires only half the number of parameters but four times the depth, suggesting that the dilated fully convolutional block can have a deeper architecture than the conventional fully convolutional filter when the total number of parameters is fixed.

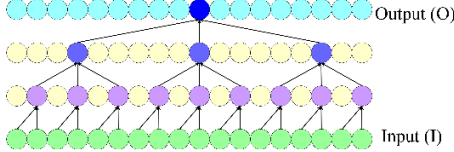


Fig. 2. Input (I) and output (O) with two-layered dilated convolutional filters.

3. THE PROPOSED MULTICHANNEL SE SYSTEM

In this section, we introduce the proposed SDFCN multichannel SE system. Then, we explain the extended system, rSDFCN. The design concept and architectures of SDFCN and rSDFCN are presented.

3.1 SDFCN System

Fig. 3 shows the architecture of the proposed SDFCN multichannel SE system, which consists of a SincConv layer and a dilated FCN (termed DFCN) module. The DFCN module consists of four layers of dilated convolutional blocks (Dilated Conv Block in Fig. 3), four dilated convolutional layers, and a tanh activation function layer. A skip-connection scheme is adopted in the first and second dilated convolutional blocks to provide additional information to the higher-level process. From our preliminary experimental results, we note that with such a skip-connection scheme, the SDFCN model can be trained more efficiently. Given the multichannel inputs: $\mathbf{Y} = [y_1, y_2, \dots, y_N]$, where N denotes the number of channels, we have

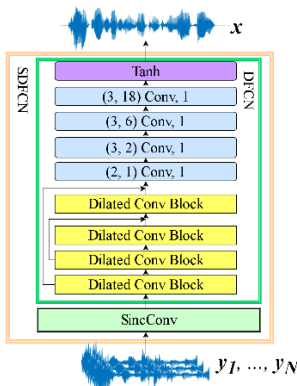


Fig. 3. Architecture of SDFCN multichannel SE system. Each of four blue rectangles denotes one dilated convolutional layer, and parameters are denoted as follows: (p_1, p_2) Conv p_3 , where p_1 is kernel size, p_2 is dilated rate, and p_3 is filter channels of layer.

$$\mathbf{x} = f_{\text{DFCN}}(f_{\text{SincCov}}(\mathbf{Y})) \quad (3)$$

where $f_{\text{SincCov}}(\cdot)$ and $f_{\text{DFCN}}(\cdot)$ denote the mapping functions of the SincCov layer and the DFCN module, respectively.

Fig. 4 shows the architecture of the dilated convolutional blocks (Dilated Conv Block in Fig. 3) in the SDFCN model. The block consists of four layers of dilated convolutional layers (the four blue rectangles) followed by batch normalization and LeakyRelu.

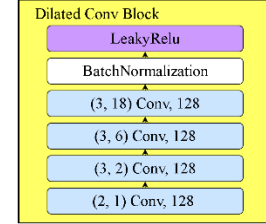


Fig. 4. Architecture of dilated convolutional block in SDFCN model.

3.2 Residual SDFCN (rSDFCN) System

Recently, residual structures have been popularly used in neural network models to attain better classification and regression efficacy. In speech signal generation tasks, residual connections also provide promising performance because the residuals (differences) of the estimated and reference signals are generally easier to model. By passing the low-level information to advanced processing, the model only needs to estimate and compensate for the residual components of the processed speech signals. Here, we also explore the combination of the residual structures with SDFCN. This combined model is termed a residual SDFCN (rSDFCN). The architecture of an rSDFCN multichannel SE system is shown in Fig. 5. As can be seen from the figure, an additional SE module (the pre-trained FCN in Fig. 5) is used. This SE module is treated as the primary SE module, and the output of the primary SE module is combined with the output of the SDFCN system to form the final enhanced output. The formulation of the rSDFCN can be represented as:

$$\mathbf{x} = f_{\text{DFCN}}(f_{\text{SincCov}}(\mathbf{Y}), f_{\text{Pr}}(\mathbf{Y})) + f_{\text{Pr}}(\mathbf{Y}) \quad (4)$$

where $f_{\text{Pr}}(\cdot)$ is the mapping function of the primary SE module.

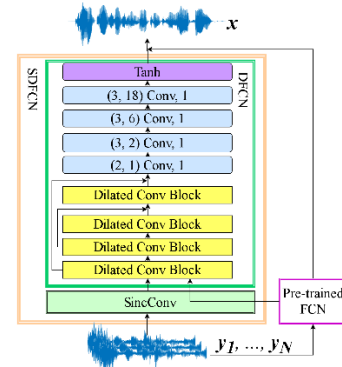


Fig. 5. Architecture of rSDFCN multichannel SE system, which consists of primary SE module (pretrained FCN) and SDFCN system.

When implementing the rSDFCN system, we first pretrain the primary SE module (fixed or not) and then train the SDFCN system. In this way, the SDFCN system learns the residual components (or differences) of the clean reference and the enhanced output of the primary SE module. More specifically, the SDFCN system is trained with the aim of minimizing the following loss function:

$$\|f_{\text{SDFCN}}(f_{\text{SincCov}}(\mathbf{Y}), f_{\text{Ax}}(\mathbf{Y})) - [\mathbf{x} - f_{\text{Ax}}(\mathbf{Y})]\|^2 \quad (5)$$

In this paper, we use a pretrained FCN model as the primary SE module. Its architecture is shown in Fig. 6. The module consists of seven layers of convolution blocks, a convolutional layer, and a tanh activation function layer. Each convolution block consists of a convolutional layer (with length = 55 and channel = 30), batch normalization, and LeakyReLU.

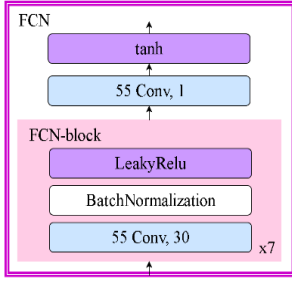


Fig. 6. Architecture of the FCN model that is used as the primary SE module in the proposed rSDFCN system. We use p_1 Conv p_2 to represent a convolutional layer with kernel size of p_1 and filter channels of p_2 .

4. EXPERIMENTAL SETUP AND RESULTS

In this section, we first introduce the experimental setup for the two multichannel SE tasks. Then, we present and discuss the results of the proposed SDFCN and rSDFCN systems for these two tasks.

4.1. Experimental Setup

In the following two subsections, we first describe the experimental setup of the IEM-SE and DM-SE tasks. We evaluated the SE performance in terms of two standard objective metrics: STOI [47], [48] and PESQ [49]. The STOI score ranges from 0 to 1, and the PESQ score ranges from 0.5 to 4.5. For STOI and PESQ, a higher score indicates that the enhanced speech signal has higher intelligibility and better quality, respectively, with reference to the speech signal recorded by the near-field high-quality microphone. In addition, we also evaluated the speech recognition performance of enhanced speech in terms of the Chinese character error rate (CER) using Google Speech Recognition [55].

For comparison, we implemented a DDAE-based multichannel SE system [17], [18]. In previous studies, the single-channel DDAE approach has shown outstanding performance in noise reduction [56], dereverberation [57], and bone-conducted speech enhancement [58]. Here, we extended the original single-channel DDAE approach to form a multichannel DDAE system. Fig. 7 shows the architecture of the multichannel DDAE system, which consists of five dense layers. The input is multiple sequences of noisy spectral features [log-power spec-

rogram (LPS) in this study] from the multiple channels, and the output is a sequence of enhanced spectral features. The phase of one of the noisy speech utterances was used as the phase to reconstruct the enhanced waveform. All neural network models were trained using the Adam optimizer [59] with a learning rate of 0.001 and the α value of LeakyReLU set to 0.3.

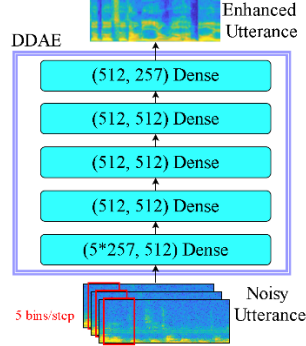


Fig. 7. Architecture of DDAE multichannel SE system.

4.2. IEM-SE Task

When speech signals are recorded using inner-ear microphones, interference from the environment can be blocked, so that purer signals can be captured. However, owing to the different transmission pathways, the speech signals captured by the IEMs exhibit different characteristics from those recorded by normal air-conducted microphones (ACMs). Generally speaking, the high-frequency components of speech recorded by an IEM are suppressed, thereby notably degrading the speech quality and intelligibility. Moreover, owing to the loss of high-frequency components, the IEM speech cannot provide a satisfactory ASR performance.

For the IEM-SE task, we intend to transform the speech signals captured by a pair of IEMs into ACM-like speech signals with improved quality and intelligibility. In the past, there have been some studies on IEM-to-ACM transformation. In [60] and [61], bandwidth expansion and equalization techniques were used to map the IEM speech signals to the ACM ones. Because the mapping function between IEM and ACM is nonlinear and complex, traditional linear filters may not provide optimal performance. In the present study, we propose to perform multichannel SE in the waveform domain for IEM-ACM transformation.

Our recording condition is shown in Fig. 8. A male speaker sat in a sound booth and wore a pair of IEMs and a near-mouth ACM. The three microphones simultaneously recorded speech signals spoken by the male speaker. The recording scripts were the Taiwan Mandarin Chinese version of Hearing in Noise Test (TMHINT) sentences [62]. There were 250 utterances for training and another 50 utterances for testing. All utterances were sampled and normalized at 16,000 Hz and truncated to 36,500 sample points (about 2.28 s).

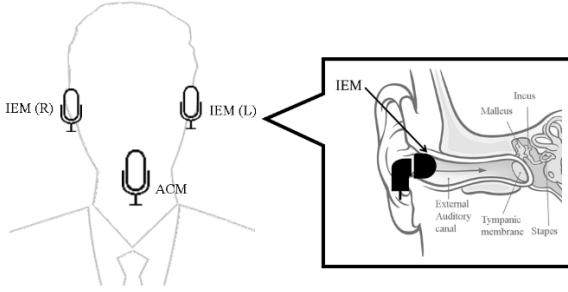


Fig. 8. Recording setting of IEM-SE task. There is a near-mouth microphone and two IEMs in both ears.

Table I lists the average STOI and PESQ scores of the original speech signals captured by the left and right IEMs [denoted as IEM (L) and IEM (R), respectively] and the enhanced speech signal by the proposed multichannel SDFCN SE method. The corresponding ACM speech was used as the reference to compute the scores. To investigate the effectiveness of using multiple (dual) channels, we first experimented with the same SDFCN model with only one-channel of noisy speech as input. The results are denoted as SDFCN (L) and SDFCN (R) in Table I. From the table, we first note that SDFCN (L) and SDFCN (R) achieve improved STOI and PESQ scores over IEM (L) and IEM (R), respectively. The results confirm the effectiveness of the proposed SDFCN system for single microphone SE. Next, we note that SDFCN (using dual channel inputs) outperforms both SDFCN (L) and SDFCN (R), confirming the advantage of multichannel (dual channel) over its single-channel counterpart.

TABLE I
AVERAGE STOI AND PESQ SCORES OF SINGLE-CHANNEL AND MULTICHANNEL SE MODELS FOR IEM-SE TASK.

No. of ch.	1	1	1	1	2
Model	IEM (L)	IEM (R)	SDFCN (L)	SDFCN (R)	SDFCN
STOI	0.694	0.694	0.861	0.824	0.880
PESQ	1.146	1.101	1.631	1.597	1.643

Next, we report the results of rSDFCN in Table II. To confirm the effectiveness of SincConv, we tested the results of replacing the SincConv layer in SDFCN with a normal convolutional layer; the results are listed as DFCN. FCN denotes the results of the pre-trained FCN module used in rSDFCN. Comparing the results of SDFCN in Table I and the results of DFCN in Table II, we confirm the effectiveness of SincConv for the SE task. Comparing the results of SDFCN in Table I and the results of FCN and rSDFCN in Table II, we confirm the effectiveness of the residual architecture for the SE task. Next, we note that both SDFCN and rSDFCN outperform the baseline DDAE system, and rSDFCN outperforms SDFCN.

TABLE II
AVERAGE STOI AND PESQ SCORES OF DIFFERENT MULTICHANNEL SE MODELS FOR IEM-SE TASK.

No. of ch.	2	2	2	2
Model	DFCN	FCN	DDAE	rSDFCN
STOI	0.867	0.834	0.773	0.894
PESQ	1.562	1.446	1.939	1.986

In addition to comparing the objective scores, we also conducted qualitative analysis. Fig. 9 (a), (b), (c), (d), and (e) show the waveforms and spectrograms of the near-field ACM, IEM (L), and IEM (R) speech signals and the enhanced speech signals obtained by rSDFCN and DDAE, respectively. By comparing Fig. 9 (a), (b), and (c), we can easily note that the IEM speech signals suffer notable distortion, with high-frequency components being suppressed. Next, by comparing Fig. 9 (a) and (d), we note that the proposed rSDFCN multichannel SE approach can generate an enhanced speech signal similar to the ACM recorded speech signal. We can also observe that the DDAE-enhanced speech signal has a clearer structure in the high-frequency components while exhibiting some distortion in the low-frequency components.

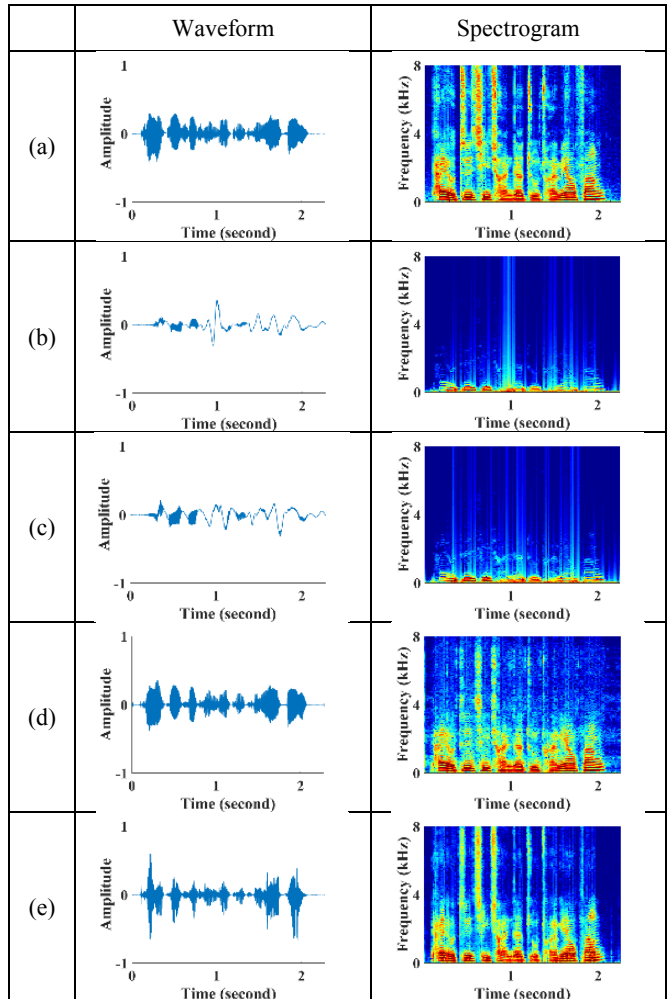


Fig. 9. Waveforms and spectrograms of an example utterance in the IEM-SE task: (a) recorded speech by near-mouth microphone; (b) and (c) recorded speech by right and left IEMs; (d) and (e) enhanced speech by rSDFCN and DDAE, respectively.

To subjectively evaluate the perceptual quality of the enhanced speech, we conducted AB reference test to compare the proposed rSDFCN with the original IEM speech (here IEM(L) was used since it gave slightly higher PESQ scores as shown in Table I). For comparison, the DDAE enhanced speech were also involved in the preference test. Accordingly, three pairs of listening tests were conducted, namely rSDFCN versus IEM, DDAE versus IEM, and

rSDFCN versus DDAE. Each pair of speech samples were presented in a randomized order. For each listening test, speech samples were randomly selected from the test set, and 15 listeners participated. Listeners were instructed to select the speech sample with better quality. The stimuli were played to the listeners in a quiet environment through a set of Sennheiser HD headphones at a comfortable listening level. From Fig. 10 (a) and (b), both rSDFCN and DDAE clearly outperform IEM (L) with notable margins, confirming the effectiveness of these two SE approaches. Next from Fig. 10 (c), we note that rSDFCN yield a higher preference score as compared to DDAE, showing that rSDFCN can more effectively enhance the IEM speech.

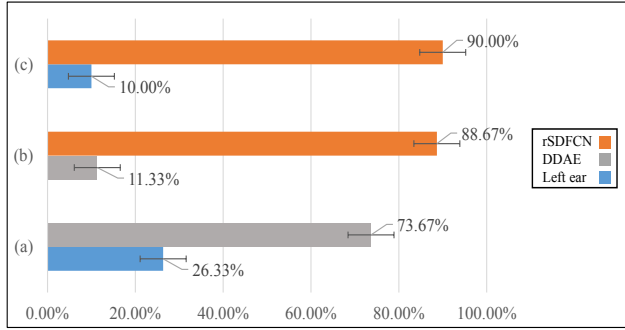


Fig. 10. Results of AB preference test (with 95% confidence intervals) on speech quality compared between proposed rSDFCN and IEM (L) and DDAE for the IEM-SE task.

Finally, we tested the ASR performance in terms of the character error rate (CER). The results of the speech recorded by ACM, IEM, IEM (L), and IEM (R) and the enhanced speech by the rSDFCN and DDAE are shown in Fig. 11. The CER of the ACM-recorded speech is 9.2%, which can be regarded as the upper-bound. The CERs of the speech recorded by IEM (L) and IEM (R) and the enhanced speech by rSDFCN and DDAE are 26.9%, 26.0%, 16.8%, and 28.6%, respectively. From the results, we can note that rSDFCN can improve the ASR performance over IEM (L) and IEM (R). Compared with IEM (L), CER decreased by 35.38 % (from 26.0% to 16.8%). Comparing the results in Fig. 10 and 11 and Table II, we note that rSDFCN outperforms DDAE in terms of PESQ, STOI, subjective preference test scores, and ASR results, confirming the effectiveness of the proposed rSDFCN over the conventional DDAE approach for the IEM-SE task.

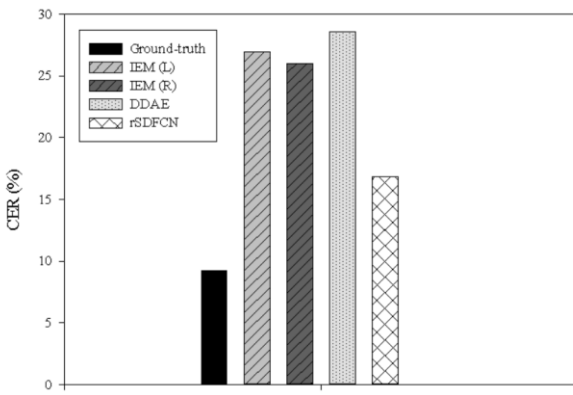


Fig. 11. ASR results achieved by different SE models for IEM-SE task.

4.3. DM-SE Task

For the DM-SE task, we also used the scripts of the TMHINT sentences to prepare the speech dataset. The layout of the recording is shown in Fig. 12. A high-quality near-field microphone (Shure PGA181 [63]) was placed right in front of the speaker and five low-quality microphones (all of the same brand and model: Sanlux HMT-11 [64]) were located at the five vertices of the regular hexagon, 1 m away from the speaker. We labeled the low-quality microphones in counterclockwise order from I to V starting from the microphone in front of the speaker.

Herein, the goal was to generate an enhanced (high-quality) speech signal using the speech signals recorded by the distant and low-quality microphones. To validate the effectiveness of using multiple channels for SE, we designed seven scenarios: five single-channel SE scenarios where the input consisted of the speech signal recorded by one of the five microphones [(I), (II), (III), (IV), or (V)] and the output was the enhanced speech signal, and two multichannel SE scenarios, where the input consisted of the speech signals recorded by three microphones (I, II, and V) and five microphones (I, II, III, IV, and V) and the output was the enhanced speech signal. For this set of experiments, we used 250 utterances for training and another 50 utterances for testing. All utterances were sampled and normalized at 16,000 Hz and truncated to 36,500 sample points (about 2.28 s).

It is worth noting that although both IEM- and DM-SE tasks are multichannel SE scenarios, there are clear differences between them. For an IEM-SE task, the high-frequency components of the IEM speech signals are suppressed. In other words, the IEM speech resembles the low-pass-filtered ACM speech. Meanwhile, for the DM-SE task, the speech signals recorded by microphones I, II, III, IV, and V were degraded versions of the speech recorded by the near-field microphone owing to low-quality recording hardware, long-range fading, and room reverberation. As with the IEM-SE task, we tested the performance of rSDFCN and DDAE.

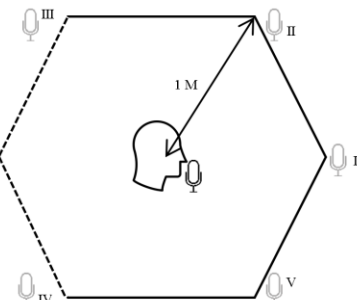


Fig. 12. Recording setting for DM-SE task. There is a near-field high-quality microphone and five far-field low-quality microphones. Distances of near-field microphone to far-field microphones are all 1 m.

Tables III and IV respectively show the average STOI and PESQ scores of rSDFCN and DDAE under seven conditions. The scores of the speech recorded by the far-field microphone (using the corresponding speech recorded by the near-field microphone as a reference) are also listed for comparison. From the tables, we can easily see that both SE models can improve the STOI and PESQ scores over the seven conditions. When only one input is available

TABLE III
AVERAGE STOI SCORES OF rSDFCN AND DDAE FOR DM-SE TASK.

STOI		LPS	RWF
Input Microphone(s)	Baseline	DDAE	rSDFCN
I	0.872	0.823	0.932
II	0.888	0.814	0.930
III	0.896	0.813	0.931
V	0.881	0.813	0.931
VI	0.893	0.816	0.931
I, II, VI		0.823	0.950
I, II, III, V, VI		0.829	0.954

TABLE IV
AVERAGE PESQ SCORES OF rSDFCN AND DDAE FOR DM-SE TASK.

PESQ		LPS	RWF
Input Microphone(s)	Baseline	DDAE	rSDFCN
I	1.602	1.618	1.648
II	1.736	1.606	1.656
III	1.526	1.623	1.644
V	1.495	1.581	1.642
VI	1.727	1.581	1.646
I, II, VI		1.655	1.780
I, II, III, V, VI		1.635	1.826

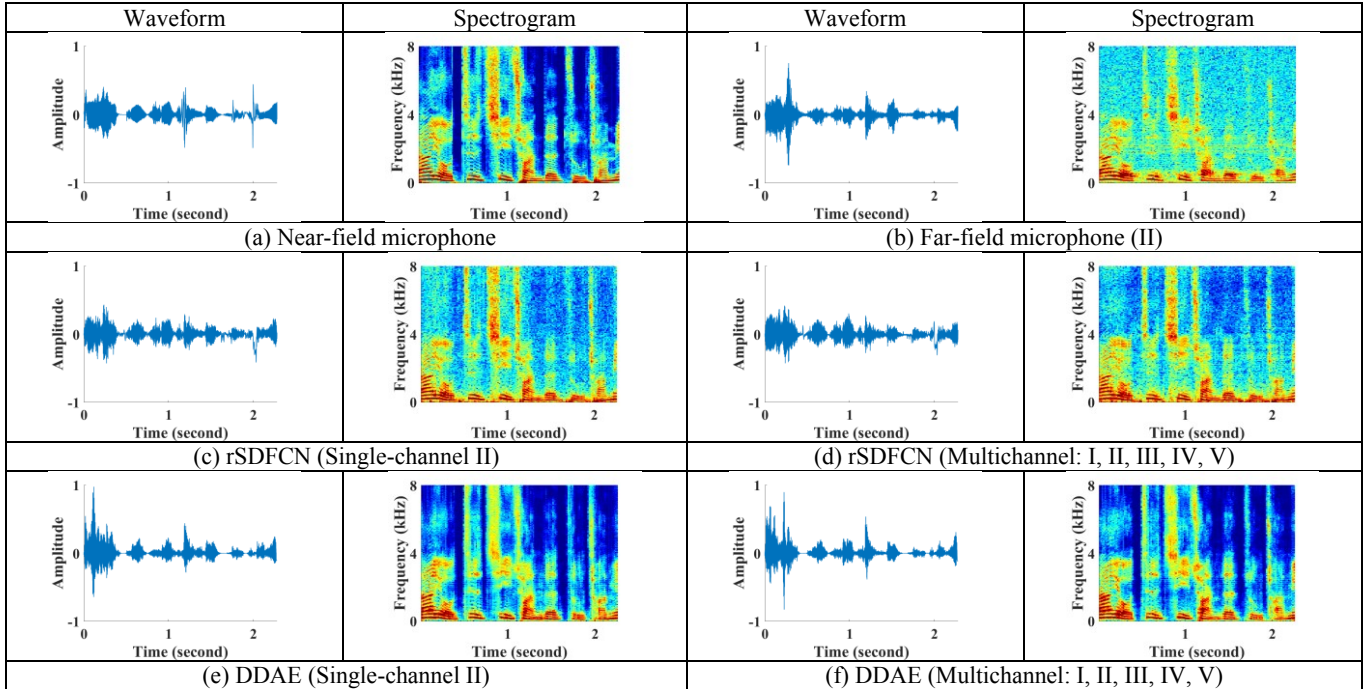


Fig. 13. Waveforms and spectrograms of example utterance in DM-SE task: (a) speech recorded by near-field microphone; (b) speech recorded by second far-field microphone (channel II); (c) and (e) enhanced speech by rSDFCN and DDAE with single-channel input; (d) and (f) enhanced speech by rSDFCN and DDAE with five channels of input.

(the task becomes a single-channel SE task), rSDFCN outperforms DDAE consistently in five cases with a single far-field microphone (I, II, III, IV, and V). Meanwhile, for the multichannel task (I, II, VI) and {I, II, III, V, VI}), rSDFCN also outperforms DDAE. In addition, it is clear that the results of multichannel SE are superior to those of single-channel SE, implying that multichannel signals

can provide more useful information for model learning.

For qualitative analysis, the waveforms and spectrograms of a speech utterance recorded by the near-field microphone and the far-field microphone (channel II), along with the enhanced speech from rSDFCN and DDAE are shown in Fig. 13. Owing to space constraints, for multichannel SE, we only display the waveforms

and spectrograms of the enhanced speech using five channels ({I, II, III, V, and VI}). By comparing Fig. 13 (d) and (f), we can observe that DDAE is superior to rSDFCN, providing a relatively clear structure for spectrogram restoration; by contrast, rSDFCN outperforms DDAE when observing the waveform. This result is reasonable because DDAE aims to minimize the mean square error (MSE) in the spectral domain, while rSDFCN aims to minimize the MSE in the waveform domain.

We also conducted listening tests to compare the proposed rSDFCN method with the DDAE and the second far-field microphone (channel II, which achieved the highest PESQ score, as shown in Table IV). The results are shown in Fig. 14. From Fig. 14 (a), we note dissimilar results from those in Fig. 10 (a): DDAE cannot improve the speech quality effectively. A possible reason is that the distortions caused by distance did not affect the speech quality too much. Thus, although the DDAE approach can recover missing speech signal components, it may generate distortions and accordingly deteriorate the speech quality. From Fig. 14 (b), we note that the rSDFCN can yield higher speech quality scores than the DDAE, confirming that rSDFCN is superior to DDAE in terms of subjective listening tests. Finally, from Fig. 14 (c), we note that the rSDFCN enhanced speech and the one recorded by the second far-field microphone are comparable (50.71% versus 49.29%).

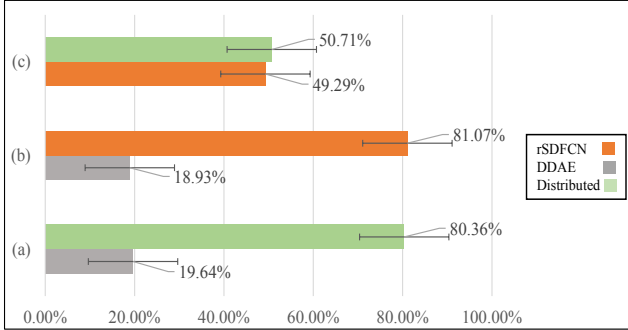


Fig. 14. Results of AB preference test (with 95% confidence intervals) on speech quality compared between proposed rSDFCN and IEM (L) and DDAE for the DM-SE task.

The recognition results using Google ASR are shown in Fig. 15. We report the performance of the speech recorded by the near-field microphone (as the upper-bound) and the second far-field microphone (channel II, which achieved the best ASR results in our experiments) and the enhanced speech by DDAE and rSDFCN. The corresponding CERs are 9.8%, 14.4%, 18%, and 10.4%. From the CERs in Fig. 15, we first note a clear drop in ASR performance from near-field microphone speech to far-field microphone speech. Next, we note that the CER of the rSDFCN enhanced speech (10.4%) is much lower than that of the far-field microphone speech (14.0%) and close to that of the near-field microphone speech (9.8%). The rSDFCN multichannel SE system reduced the CER by 27.8 % (from 14.4 % to 10.4 %) compared to the unenhanced single-channel far-field microphone speech. Comparing the results in Fig. 14 and 15 and Tables III and IV, we note that rSDFCN outperforms DDAE in terms of PESQ, STOI, subjective preference test scores, and ASR results, confirming the effectiveness of the proposed rSDFCN over the conventional DDAE approach for the DM-SE task.

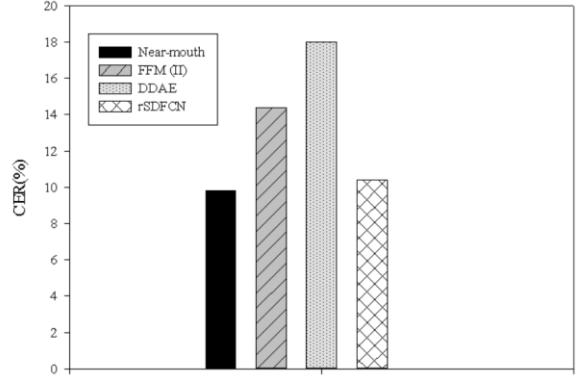


Fig. 15. ASR results achieved by different SE models for DM-SE task.

6. CONCLUSION

In this paper, we proposed the SDFCN waveform-mapping-based multichannel SE system and an extended version, rSDFCN, to further improve the performance. We tested the proposed SE systems on two multichannel SE tasks: IEM-SE and DM-SE. The experimental results for both tasks confirmed the effectiveness of the proposed systems in achieving higher STOI and PESQ scores, as well as providing improved ASR performance. The proposed waveform-based rSDFCN SE system outperformed the spectrogram-based DDAE SE system, which means that phase information is important for multichannel SE.

To the best of our knowledge, this study is the first to adopt the concept of waveform mapping based on neural network models to enhance multichannel speech signals under noisy conditions. In this work, both IEM-SE and DM-SE tasks simulated a “virtual” high-performance and near-field microphone to overcome the distortion caused by channel effects and spatial fading, and to attain improved speech quality (PESQ), speech intelligibility (STOI), subjective listening scores, and ASR performance. Please note that different from the beamforming methods that require spatial and time-delay information, this study investigates the scenario where the speech signals are recorded by multiple microphones simultaneously. In the future, we will extend the proposed systems to multichannel tasks where multiple distortion factors including noise, interference, and reverberation are involved. Meanwhile, we will explore the possibility of combining the advantages of waveform-mapping- and spectral-mapping-based multichannel SE methods to further improve our current systems.

6. REFERENCE

- [1] Z. Zhao, H. Liu, and T. Fingscheidt, “Convolutional neural networks to enhance coded speech,” *IEEE/ACM Transactions on Audio, Speech, and Language Processing*, vol. 27, no. 4, pp. 663-678, 2019.
- [2] J. Li *et al.*, “Comparative intelligibility investigation of single-channel noise-reduction algorithms for Chinese, Japanese, and English,” *J. Acoust. Soc. Am.*, vol. 129, no. 5, pp. 3291–3301, 2011.
- [3] J. Chen, Y. Wang, S. E. Yoho, D. Wang, and E. W. Healy, “Large-scale training to increase speech intelligibility for hearing-impaired listeners in novel noises,” *J. Acoust. Soc. Am.*, vol. 139, no. 5, pp. 2604-2612, 2016.

[4] Y.-H. Lai, F. Chen, S.-S. Wang, X. Lu, Y. Tsao, and C.-H. Lee, "A deep denoising autoencoder approach to improving the intelligibility of vocoded speech in cochlear implant simulation," *IEEE Trans. Biomed. Eng.*, vol. 64, no. 7, pp. 1568–1578, 2017.

[5] J. Li, L. Deng, R. Haeb-Umbach, and Y. Gong, *Robust Automatic Speech Recognition: A Bridge to Practical Applications*. Academic Press, 2015.

[6] S. Boll, "Suppression of acoustic noise in speech using spectral subtraction," *IEEE Trans. Acoust. Speech Signal Process.*, vol. 27, no. 2, pp. 113–120, 1979.

[7] J. Lim and A. Oppenheim, "All-pole modeling of degraded speech," *IEEE Trans. on Acoustics, Speech, and Signal Processing*, vol. 26, no. 3, pp. 197–210, 1978.

[8] P. Scalart and J. V. Filho, "Speech enhancement based on a priori signal to noise estimation," in *Proc. ICASSP 1996*, pp. 629–632.

[9] Y. Ephraim and D. Malah, "Speech enhancement using a minimum-mean square error short-time spectral amplitude estimator," *IEEE Trans. Acoust. Speech Signal Process.*, vol. 32, no. 6, pp. 1109–1121, 1984.

[10] H. Yu and P. C. Loizou, "A generalized subspace approach for enhancing speech corrupted by colored noise," *IEEE Trans. Speech Audio Process.*, vol. 11, no. 4, pp. 334–341, 2003.

[11] A. Rezayee and S. Gazor, "An adaptive KLT approach for speech enhancement," *IEEE Trans. Speech Audio Process.*, vol. 9, no. 2, pp. 87–95, 2001.

[12] R. Vetter, N. Virág, P. Reneyev, and J.-M. Vesin, "Single channel speech enhancement using principal component analysis and MDL subspace selection," in *Proc. EUROSPEECH 1999*.

[13] N. Mohammadiha, P. Smaragdis, and A. Leijon, "Supervised and unsupervised speech enhancement using nonnegative matrix factorization," *IEEE Trans. Audio Speech Lang. Process.*, vol. 21, no. 10, pp. 2140–2151, 2013.

[14] J. Wang, Y. Lee, C. Lin, S. Wang, C. Shih, and C. Wu, "Compressive sensing-based speech enhancement," *IEEEACM Trans. Audio Speech Lang. Process.*, vol. 24, no. 11, pp. 2122–2131, 2016.

[15] C. D. Sigg, T. Dikk, and J. M. Buhmann, "Speech enhancement with sparse coding in learned dictionaries," in *Proc. ICASSP 2010*, pp. 4758–4761.

[16] P. Huang, S. D. Chen, P. Smaragdis, and M. Hasegawa-Johnson, "Singing-voice separation from monaural recordings using robust principal component analysis," in *Proc. ICASSP 2012*, pp. 57–60.

[17] X. Lu, Y. Tsao, S. Matsuda, and C. Hori, "Ensemble modeling of denoising autoencoder for speech spectrum restoration," in *Proc. INTERSPEECH 2014*, pp. 885–889.

[18] X. Lu, Y. Tsao, S. Matsuda, and C. Hori, "Speech enhancement based on deep denoising autoencoder," in *Proc. INTERSPEECH 2013*, pp. 436–440.

[19] M. Kolbæk, Z. Tan, and J. Jensen, "Speech intelligibility potential of general and specialized deep neural network based speech enhancement systems," *IEEEACM Trans. Audio Speech Lang. Process.*, vol. 25, no. 1, pp. 153–167, 2017.

[20] D. Liu, P. Smaragdis, and M. Kim, "Experiments on deep learning for speech denoising," in *Proc. INTERSPEECH 2014*, pp. 2685–2689.

[21] Y. Xu, J. Du, L. Dai, and C. Lee, "An experimental study on speech enhancement based on deep neural networks," *IEEE Signal Process. Lett.*, vol. 21, no. 1, pp. 65–68, 2014.

[22] Y. Xu, J. Du, L. Dai, and C. Lee, "A regression approach to speech enhancement based on deep neural networks," *IEEEACM Trans. Audio Speech Lang. Process.*, vol. 23, no. 1, pp. 7–19, 2015.

[23] P. Campolucci, A. Uncini, F. Piazza, and B. D. Rao, "On-line learning algorithms for locally recurrent neural networks," *IEEE Trans. Neural Netw.*, vol. 10, no. 2, pp. 253–271, 1999.

[24] F. Weninger, F. Eyben, and B. Schuller, "Single-channel speech separation with memory-enhanced recurrent neural networks," in *Proc. ICASSP 2014*, pp. 3709–3713.

[25] S.-W. Fu, T. Hu, Y. Tsao, and X. Lu, "Complex spectrogram enhancement by convolutional neural network with multi-metrics learning," in *Proc. MLSP 2017*, pp. 1–6.

[26] S.-W. Fu, Y. Tsao, and X. Lu, "SNR-aware convolutional neural network modeling for speech enhancement," in *Proc. INTERSPEECH 2016*, pp. 3768–3772.

[27] F. Eyben, F. Weninger, S. Squartini, and B. Schuller, "Real-life voice activity detection with LSTM Recurrent Neural Networks and an application to Hollywood movies," in *Proc. ICASSP 2013*, pp. 483–487.

[28] F. Weninger *et al.*, "Speech enhancement with LSTM recurrent neural networks and its application to noise-robust ASR," in *Latent Variable Analysis and Signal Separation*, vol. 9237, E. Vincent, A. Yeredor, Z. Koldovský, and P. Tichavský, Eds. Cham: Springer International Publishing, 2015, pp. 91–99.

[29] Z. Chen, S. Watanabe, H. Erdogan, and J. R. Hershey, "Speech enhancement and recognition using multi-task learning of long short-term memory recurrent neural networks," in *Proc. INTERSPEECH 2015*, pp. 3274–3278.

[30] L. Sun, J. Du, L. Dai, and C. Lee, "Multiple-target deep learning for LSTM-RNN based speech enhancement," in *Proc. HSCMA 2017*, pp. 136–140.

[31] J. Bitzer, K. U. Simmer, and K. Kammeyer, *Multi-Microphone Noise Reduction Techniques For Hands-Free Speech Recognition - A Comparative Study*. 1999.

[32] Q.-Liu, B. Champagne, and P. Kabal, "Room speech dereverberation via minimum-phase and all-pass component processing of multi-microphone signals," in *Proc. PacRim 1995*, pp. 571–574.

[33] O. Hoshuyama, A. Sugiyama, and A. Hirano, "A robust adaptive beamformer for microphone arrays with a blocking matrix using constrained adaptive filters," *IEEE Trans. Signal Process.*, vol. 47, no. 10, pp. 2677–2684, 1999.

[34] N. Yousefian and P. Loizou, "A dual-microphone speech enhancement algorithm based on the coherence function," *IEEE Trans. Audio Speech Lang. Process.*, vol. 20 (2), pp. 599–609, 2011.

[35] and T. Kailath, "Adaptive beamforming for coherent signals and interference," *IEEE Trans. Acoust. Speech Signal Process.*, vol. 33, no. 3, pp. 527–536, 1985.

[36] X. Li, M. Fan, L. Liu, and W. Li, "Distributed-microphones based in-vehicle speech enhancement via sparse and low-rank spectrogram decomposition," *Speech Commun.*, vol. 98, pp. 51–62, 2018.

[37] P. Vincent, H. Larochelle, Y. Bengio, and P.-A. Manzagol, "Extracting and composing robust features with denoising autoencoders," in *Proc. ICML 2008*, pp. 1096–1103.

[38] S. Araki, T. Hayashi, M. Delcroix, M. Fujimoto, K. Takeda, and T. Nakatani, "Exploring multi-channel features for de-

noising-autoencoder-based speech enhancement,” in *Proc. ICASSP 2015*, pp. 116–120.

[39] Z.-Q. Wang and D. Wang, “All-neural multi-channel speech enhancement,” in *Proc. Interspeech 2018*, pp. 3234–3238.

[40] S.-W. Fu, Y. Tsao, X. Lu, and H. Kawai, “Raw waveform-based speech enhancement by fully convolutional networks,” in *Proc. APSIPA 2017*, pp. 6–12, 2017.

[41] S.-W. Fu, T.-W. Wang, Y. Tsao, X. Lu, and H. Kawai, “End-to-end waveform utterance enhancement for direct evaluation metrics optimization by fully convolutional neural networks,” *IEEE/ACM Trans. Audio Speech Lang. Process.*, vol. 26, no. 9, pp. 1570–1584, 2018.

[42] S. Pascual, A. Bonafonte, and J. Serra, “SEGAN: Speech enhancement generative adversarial network,” in *Proc. INTERSPEECH*, 2017, pp. 3642–3646.

[43] D. Rethage, J. Pons, and X. Serra, “A Wavenet for speech denoising,” in *Proc. ICASSP 2018*, pp. 5069–5073.

[44] K. Qian, Y. Zhang, S. Chang, X. Yang, D. Florêncio, and M. Hasegawa-Johnson, “Speech enhancement using Bayesian Wavenet,” in *Proc. INTERSPEECH 2017*, pp. 2013–2017.

[45] E. M. Grais, H. Wierstorf, D. Ward, and M. D. Plumbley, “Multi-resolution fully convolutional neural networks for monaural audio source separation,” in *Proc. LVA/ICA 2018*, pp. 340–350.

[46] E. M. Grais, D. Ward, and M. D. Plumbley, “Raw multi-channel audio source separation using multi-resolution convolutional auto-encoders,” in *Proc. EUSIPCO 2018*, pp. 1577–1581.

[47] C. H. Taal, R. C. Hendriks, R. Heusdens, and J. Jensen, “A short-time objective intelligibility measure for time-frequency weighted noisy speech,” in *Proc. ICASSP 2010*, pp. 4214–4217.

[48] C. H. Taal, R. C. Hendriks, R. Heusdens, and J. Jensen, “An algorithm for intelligibility prediction of time–frequency weighted noisy speech,” *IEEE Trans. Audio Speech Lang. Process.*, vol. 19, no. 7, pp. 2125–2136, 2011.

[49] A. W. Rix, J. G. Beerends, M. P. Hollier, and A. P. Hekstra, “Perceptual evaluation of speech quality (PESQ)-a new method for speech quality assessment of telephone networks and codecs,” in *Proc. ICASSP 2001*, pp. 749–752.

[50] A. van den Oord *et al.*, “WaveNet: A generative model for raw audio,” *ArXiv160903499 Cs*, Sep. 2016.

[51] M. Ravanelli and Y. Bengio, “Speaker recognition from raw waveform with SincNet,” *ArXiv180800158 Cs Eess*, Jul. 2018.

[52] Y. Luo and N. Mesgarani, “Conv-TasNet: surpassing ideal time-frequency magnitude masking for speech separation,” *IEEE Trans. Audio Speech Lang. Process.*, vol. 27 (8), pp. 1256–1266, 2018.

[53] C. Donahue, J. McAuley, and M. Puckette, “Adversarial audio synthesis,” in *Proc. ICLR 2019*.

[54] F. Yu and V. Koltun, “Multi-scale context aggregation by dilated convolutions,” in *Proc. ICLR 2016*.

[55] A. Zhang, *Speech Recognition (Version 3.8) [Software]*. Available from https://github.com/Uberi/speech_recognition#readme, 2017.

[56] Y.-H. Lai *et al.*, “Deep learning-based noise reduction approach to improve speech intelligibility for cochlear implant recipients:,” *Ear and Hearing*, vol. 39, no. 4, pp. 795–809, 2018.

[57] W.-J. Lee, S.-S. Wang, F. Chen, X. Lu, S.-Y. Chien, and Y. Tsao, “Speech dereverberation based on integrated deep and ensemble learning algorithm,” in *Proc. ICASSP 2018*, pp. 5454–5458.

[58] H.-P. Liu, Y. Tsao, and C.-S. Fuh, “Bone-conducted speech enhancement using deep denoising autoencoder,” *Speech Commun.*, vol. 104, pp. 106–112, 2018.

[59] D. P. Kingma and J. Ba, “Adam: A method for stochastic optimization,” in *Proc. ICLR 2015*.

[60] K. Kondo, T. Fujita, and K. Nakagawa, “On equalization of bone conducted speech for improved speech quality,” in *Proc. ISSPIT 2006*, pp. 426–431.

[61] R. E. Bouserhal, T. H. Falk, and J. Voix, “In-ear microphone speech quality enhancement via adaptive filtering and artificial bandwidth extension,” *J. Acoust. Soc. Am.*, vol. 141, no. 3, pp. 1321–1331, 2017.

[62] L. L. N. Wong, S. D. Soli, S. Liu, N. Han, and M.-W. Huang, “Development of the Mandarin hearing in noise test (MHINT),” *Ear and Hearing*, vol. 28, no. Supplement, pp. 70S–74S, 2007.

[63] “PGA181 - Side-Address Cardioid Condenser Microphone.” [Online]. Available: <https://www.shure.com/en-US/products/microphones/pga181>. [Accessed: 29-Apr-2019].

[64] “SANLUX HMT-11.” [Online]. Available: http://www.sanyo.com.tw/s1504/sanyo_in_b.asp?model=2033. [Accessed: 29-Apr-2019].